Robotica (1998) volume 16, pp. 607–613. Printed in the United Kingdom © 1998 Cambridge University Press

Modeling and control of a mobile manipulator

J.H. Chung and S.A. Velinsky

Department of Mechanical and Aeronautical Engineering, University of California at Davis, Davis, CA 95616 (USA)

(Received in Final Form: May 23, 1998)

SUMMARY

This paper concerns the modeling and control of a mobile manipulator which consists of a robotic arm mounted upon a mobile platform. The equations of motion are derived using the Lagrange-d'Alembert formulation for the nonholonomic model of the mobile manipulator. The dynamic model which considers slip of the platform's tires is developed using the Newton-Euler method and incorporates Dugoff's tire friction model. Then, the tracking problem is investigated by using a well known nonlinear control method for the nonholonomic model. The adverse effect of the wheel slip on the tracking of commanded motion is discussed in the simulation. For the dynamic model, a variable structure control approach is employed to minimize the harmful effect of the wheel slip on the tracking performance. The simulation results demonstrate the effectiveness of the proposed control algorithm.

KEYWORDS: Nonholonomic model; Dynamic model; Mobile manipulator; Robust control.

1. INTRODUCTION

In recent years, there has been great effort made in the development of tracking control algorithms of wheeled mobile robots as nonholonomic systems that arise from constraining the wheels of the robots to roll without slipping. Most of the tracking control algorithms developed in the literature are based on ideal models in which nonholonomic motion is assumed. Interest in the area of mobile manipulators has also increased significantly because of their combined mobility and manipulability. Although considerable amounts of research and development have been performed in the area of motion control of mobile manipulators, most of the models developed in the previous work assume only planar motion and/or holonomic constraints in which the complexity of the modeling and control problem is often excessively simplified.

Recently, Dugoff's pneumatic tire friction model has been employed to describe the longitudinal and lateral forces acting on the wheels of a wheeled mobile robot for high load and high speed applications.[1] It was determined that the use of a nonholonomic model must be limited to lightweight vehicles which operate under very low speeds, low accelerations, and under lightly loaded conditions. This result motivates the dynamic modeling of the mobile manipulator subject to wheel slip.

Hootsmanns and Dubowsky[2] developed the mobile manipulator jacobian transpose control algorithm which relies on vehicle motion sensing and kinematic models of the system. Mobile manipulators with soft suspensions were shown to be stable with limited vehicle sensory data. However, only holonomic constraints were taken into account. Liu and Lewis[3] developed a robust controller for a mobile manipulator by considering the platform and the manipulator as two subsystems. Jang[4] studied a single-linked manipulator on a planar wheeled platform and developed passive control systems to reduce the dynamic coupling between the two subsystems. Yamamoto and Yun[5] studied a two-linked planar mobile manipulator subject to nonholonomic constraints and developed a coordination algorithm based on the concept of a preferred operating region. Chung *et al*.[6] developed the nonlinear interaction control algorithm for the redundant mobile manipulator to resolve the kinematic redundancy.

The motivation for much of other previous work[7,8] stems from identifying the stability criteria so that the vehicle does not overturn. The work addressing mobile manipulators, e.g., off-line optimization methods[9], ignores the nonholonomic characteristic of the mobile platform. Most of the models described in the previous work[2,3,5,6] analyze the dynamic interaction in an explicit form. However, they consider only planar motion and/or satisfy the assumption of holonomic motion which is far from realistic in practice.

In this paper, we first develop the nonholonomic equations of motion of a mobile manipulator using a Lagrange-d'Alembert formulation. In this formulation, the equations of motion are projected onto the subspace of allowable motions. Then, we attempt to develop the dynamic model of the spatial manipulator for high load and high speed applications, in which slip of the wheeled platform's tires is considered. Then, the solvability of tracking problems for the nonholonomic model is investigated by using input-output linearization. Furthermore, a robust control algorithm is developed for the dynamic model to minimize the harmful effect of wheel slip which is shown to act as a disturbance to the system.

2. NONHOLONOMIC MODELING

The mobile manipulator shown in Figure 1 is considered. This mobile manipulator is supported by two independently driven wheels with a common platform-fixed axis and two passive, self-aligning wheels (casters). The detailed configuration of the mobile manipulator can be found in the freebody diagrams, Figures 2 and 3, which are also used in deriving the dynamic equations of motion of the system subject to wheel slip. In this first case, the wheeled platform is modeled as a nonholonomic system in which wheel slip is

https://doi.org/10.1017/S0263574798000873 Published online by Cambridge University Press

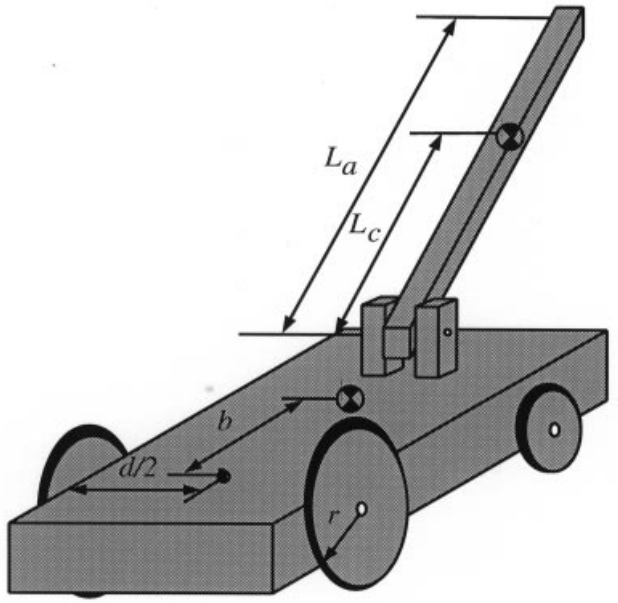


Fig. 1. The mobile manipulator.

neglected due to slow motions. Hence, we assume that no lateral slip nor longitudinal slip occurs.

The equations of motion of a system subject to constraints can be written as

$$\frac{d}{dt}\frac{\partial L}{\partial \dot{\xi}} - \frac{\partial L}{\partial \xi} + \Psi^T(\xi)\lambda - \tau = 0 \tag{1}$$

where $\Psi(\xi) \in \mathbb{R}^{k\times n}$ represents a set of k velocity constraints, $\lambda = (\lambda_1, \ldots, \lambda_k)^T$ are Lagrange multipliers, $\xi = (\xi_1, \ldots, \xi_n)^T$ are a set of generalized coordinates for the system, and L is the Lagrangian of the system.

In the absence of constraints, the robot's dynamic equations can be derived from the Euler-Lagrange equations. Given k such constraints, we can write them as a vector-valued set of k equations:

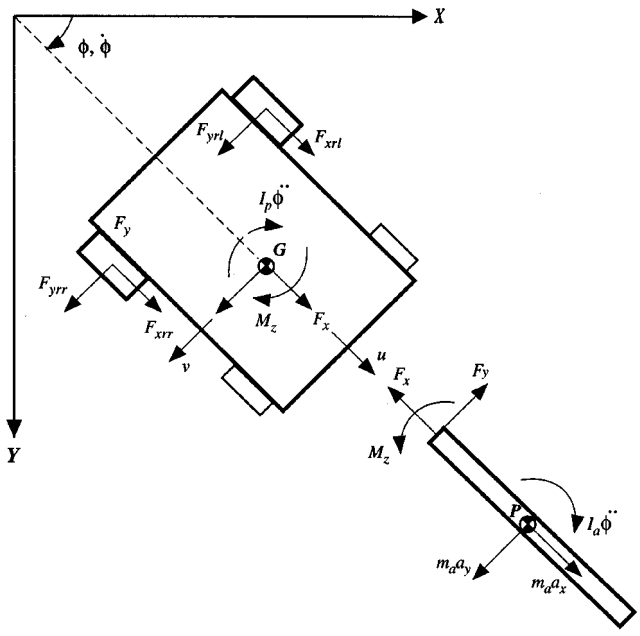


Fig. 2. Top view of the mobile manipulator.

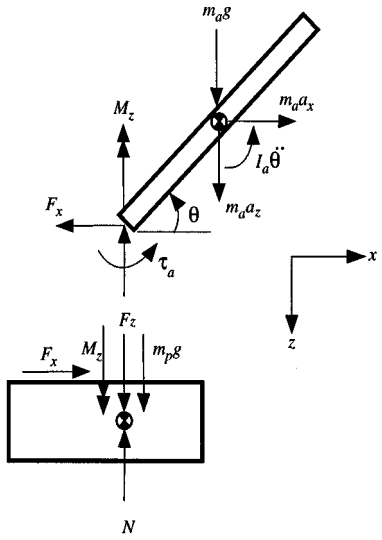


Fig. 3. Side view of the mobile manipulator.

$$\Psi_j^i(\xi)\dot{\xi} = 0, \quad i = 1, \ldots, k. \tag{2}$$

Let the virtual displacement $\delta\xi$ be a vector which satisfies $\Psi(\xi)\delta\xi = 0$. Then, $(\Psi^T(\xi)\lambda)\cdot\delta\xi = 0$ for $\Psi(\xi)\delta\xi = 0$ by D'Alembert's principle. Since $(\Psi^T(\xi)\lambda)\cdot\delta\xi = 0$, Eq. (1) becomes

$$\left(\frac{d}{dt}\frac{\partial L}{\partial \dot{\xi}} - \frac{\partial L}{\partial \xi} - \tau\right)\cdot\delta\xi = 0 \tag{3}$$

where
$$\Psi(\xi)\delta\xi = 0. \tag{4}$$

The mobile platform is subject to one holonomic constraint and two nonholonomic constraints written as

$$\phi = \frac{b}{d}(\xi_1 - \xi_2), \tag{5}$$

$$\dot{y}_m \cos\phi - \dot{x}_m \sin\phi = 0, \text{ and} \tag{6}$$

$$\dot{x}_m \cos\phi + \dot{y}_m \sin\phi = \frac{1}{2} r(\dot{\xi}_1 + \dot{\xi}_2) \tag{7}$$

where ϕ is the heading angle of the platform, (x_m, y_m) is the position coordinate of the mid-point of the axle, ξ_1 is the angular displacement of the left wheel, and ξ_2 is the angular displacement of the right wheel.

We may write Eqs. (6) and (7) in the form of Eq. (2) with a vector ξ defined as

$$\xi = [\xi_1\ \xi_2\ \xi_3\ x_m\ y_m] \tag{8}$$

where ξ_3 is the joint angle of the manipulator and $\Psi(\xi)$ is given by

$$\Psi(\xi) = \begin{bmatrix} 0 & 0 & 0 & -\sin\phi & \cos\phi \\ \frac{1}{2}r & \frac{1}{2}r & 0 & -\cos\phi & -\sin\phi \end{bmatrix}. \tag{9}$$

Substituting Eq. (6) into Eq. (7) and rearranging the resulting equations gives a set of velocity constraints

https://doi.org/10.1017/S0263574798000873 Published online by Cambridge University Press

$$\dot{x}_m = \frac{1}{2} r(\dot{\xi}_1 + \dot{\xi}_2) \cos \phi \text{ and} \tag{10}$$

$$\dot{y}_m = \frac{1}{2} r(\dot{\xi}_1 + \dot{\xi}_2) \sin \phi \tag{11}$$

Now $\Psi(\xi)$ is rearranged as

$$\Psi(\xi) = [\Psi_u(\xi) \Psi_c(\xi)] \tag{12}$$

where

$$\Psi_u(\xi) = \begin{bmatrix} 0 & 0 & 0 \\ \frac{1}{2}r & \frac{1}{2}r & 0 \end{bmatrix}, \tag{13}$$

$$\Psi_c(\xi) = \begin{bmatrix} -\sin\phi & \cos\phi \\ -\cos\phi & -\sin\phi \end{bmatrix}, \tag{14}$$

and $\Psi_c(\xi)$ is invertible and constrained.

Now, we derive the equations of motion using the Lagrange-d'Alembert formulation. Let $\delta\xi = (\delta\xi_1\ \delta\xi_2\ \delta\xi_3\ \delta x_m\ \delta y_m)$ represent a virtual displacement of the system. We obtain Eq. (3) with the set of velocity constraints as

$$\begin{bmatrix} 0 & 0 & 0 & -\sin\phi & \cos\phi \\ \frac{1}{2}r & \frac{1}{2}r & 0 & -\cos\phi & -\sin\phi \end{bmatrix} \delta\xi = 0 \tag{15}$$

Solving Eq. (15) for δx_m and δy_m gives

$$\delta x_m = \frac{1}{2} r(\delta\xi_1 + \delta\xi_2) \cos \phi \text{ and} \tag{16}$$

$$\delta y_m = \frac{1}{2} r(\delta\xi_1 + \delta\xi_2) \sin \phi. \tag{17}$$

We redefine $\delta\xi$ as $\delta\xi_u = \delta\xi_1\ \delta\xi_2\ \delta\xi_3)$ and $\delta\xi_c = (\delta x_m\ \delta y_m)$ where $\delta\xi_u$ are the set of unconstrained variables where the variables of $\delta\xi_c$ are constrained. Using Eq. (12) and $\delta\xi = (\delta\xi_u\ \delta\xi_c)$, we obtain

$$\delta\xi_c = -\Psi_c^{-T}(\xi) \Psi_u(\xi) \delta\xi_u. \tag{18}$$

It can be shown that the equations of motion become

$$\left(\frac{d}{dt} \frac{\partial L}{\partial \dot{\xi}_u} - \frac{\partial L}{\partial \xi_u} - \tau_u \right) -$$

$$\Psi_u^T \Psi_c^{-T} \left(\frac{d}{dt} \frac{\partial L}{\partial \dot{\xi}_c} - \frac{\partial L}{\partial \xi_c} - \tau_c \right) = 0. \tag{19}$$

Substituting the Lagrangian $L(\xi, \dot{\xi})$ into Eq. (19), the equations of motion of the mobile manipulator can be written as

$$D\ddot{\xi}_u + Q = \tau_u \tag{20}$$

3. DYNAMIC MODELING

In the previous section, the equations of motion of the mobile manipulator were derived based on the assumption of nonholonomic motion which is never strictly achieved in practice, especially for high load and high speed applications. By considering slip of the wheeled platform's tires, the assumption of nonholonomic motion is violated. In this section, the dynamic equations of motion are derived using the Newton-Euler method and incorporate Dugoff's nonlinear tire friction model, an empirical model that has been used for many years in the vehicle dynamics field.[10] The free-body diagrams of the mobile manipulator are shown in Figures 2 and 3. For the dynamic equations of motion derived below, the body centered frames for the platform and the manipulator are used as shown in the figures.

Given the angular velocities of the left and right wheels, ω_l and ω_r, we can write the longitudinal and lateral velocities of the center of gravity, u and v, the yaw rate ω, and the longitudinal and lateral velocities of the left and right wheels' axles, u_l and u_r as

$$u = \frac{1}{2}(u_l + u_r), \tag{21}$$

$$v = \frac{b}{d}(u_l - u_r) + v^s \tag{22}$$

$$\omega = \dot{\phi} = \frac{1}{d}(u_l - u_r), \tag{23}$$

$$u_l = r\omega_l - u_l^s, \text{ and} \tag{24}$$

$$u_r = r\omega_r - u_r^s \tag{25}$$

where ϕ is the angular displacement of the platform, v^s is the lateral slip speed of the wheel axle, u_l^s and u_r^s are the longitudinal slip speed of the centers of the left and right wheels, respectively, and r is the radius of the driving wheels. Furthermore, these equations have assumed that the platform is symmetric side-to-side such that the center of mass lies along its centerline. Using three-dimensional kinematics of rigid bodies, the acceleration of the center of mass of the manipulator can be obtained as $a_P = a_x\mathbf{i} + a_y\mathbf{j} + a_z\mathbf{k}$ where

$$a_x = \dot{u} - v\dot{\phi} - L_c\ddot{\theta} \sin\theta - L_c\dot{\theta}^2 \cos\theta - L_c\dot{\phi}^2 \cos\theta, \tag{26}$$

$$a_y = \dot{v} + u\dot{\phi} + L_c\ddot{\phi} \cos\theta - 2L_c\dot{\theta}\dot{\phi} \sin\theta, \text{ and} \tag{27}$$

$$a_z = -L_c\ddot{\theta} \cos\theta + L_c\dot{\theta}^2 \sin\theta \tag{28}$$

Using Eqs. (26)–(28), the reaction forces and moment can be obtained as follows:

$$F_x = m_a L_c \ddot{\theta} \sin\theta + m_a L_c \dot{\theta}^2 \cos\theta + m_a L_c \dot{\phi}^2 \cos\theta - m_a \dot{u} + m_a v\dot{\phi} \tag{29}$$

$$F_y = m_a L_c \dot{\theta}\dot{\phi} \sin\theta - m_a L_c \ddot{\phi} \cos\theta - m_a \dot{v} - m_a u\dot{\phi}, \text{ and} \tag{30}$$

$$M_z = m_a L_c^2 \dot{\theta}\dot{\phi} \sin\theta \cos\theta - (I_a + m_a L_c^2 \cos^2\theta)\ddot{\phi} - m_a L_c \dot{v} \cos\theta + m_a L_c v\dot{\phi} \sin\theta. \tag{31}$$

Now, the force and moment equations for the platform

https://doi.org/10.1017/S0263574798000873 Published online by Cambridge University Press

and the wheels can be written as

$$m_p(\dot{u} - v\dot{\phi}) = F_{xrl} + F_{xrr} + F_x, \tag{32}$$

$$m_p(\dot{v} + u\dot{\phi}) = F_{yrl} + F_{yrr} + F_y, \tag{33}$$

$$I_p\ddot{\phi} = M_z + \frac{d}{2}(F_{xrl} - F_{xrr}) - b(F_{yrl} + F_{yrr}), \tag{34}$$

$$(I_a + m_a L_c^2)\ddot{\theta} - m_a L_c \dot{u} \sin\theta + m_a L_c^2 \dot{\phi}^2 \sin\theta\cos\theta + m_a L_c v\dot{\phi}\sin\theta = \tau_a - m_a g L_c \cos\theta \tag{35}$$

$$I_t\dot{\omega}_l = \tau_l - F_{xrl}r, \text{ and} \tag{36}$$

$$I_t\dot{\omega}_r = \tau_r - F_{xrr}r \tag{37}$$

where m_p is the mass of the platform, m_a is the mass of the arm, I_p is the moment of the inertia of the platform about a vertical axis, and I_a is the moment of inertia of the arm about its center of mass. The distance between the center of mass of the platform and the mid-point of the axle, b, is set to zero to obtain the dynamic equations of motion in a more tractable form for the control design to follow. Note that the dynamic equations of motion are not in closed form. The longitudinal and lateral forces on the wheels are calculated by Dugoff's tire friction model.[10]

Substituting Eqs. (29)–(31) into Eqs. (32)–(35) and rearranging the resulting equations, the dynamic equations of motion of the mobile manipulator can be written as

$$M\ddot{\nu} + N + G = F \tag{38}$$

where $\ddot{\nu} = (\dot{u}\ \dot{v}\ \ddot{\phi}\ \ddot{\theta})^T$,

$$M = \begin{bmatrix} m_p + m_a & 0 & 0 & -m_a L_c \sin\theta \\ 0 & m_p + m_a & m_a L_c \cos\theta & 0 \\ 0 & m_a L_c \cos\theta & I_p + I_a + m_a L_c^2 \cos^2\theta & \\ -m_a L_c \sin\theta & 0 & 0 & I_a + m_a L_c^2 \end{bmatrix}, \tag{39}$$

$$N = \begin{bmatrix} -m_a L_c \dot{\theta}^2 \cos\theta - m_a L_c \dot{\phi}^2 \cos\theta + m_p v\dot{\phi} - m_a v\dot{\phi} \\ -m_a L_c \dot{\theta}\dot{\phi}\sin\theta + m_p u\dot{\phi} + m_a u\dot{\phi} \\ -m_a L_c^2 \dot{\theta}\dot{\phi}\sin\theta\cos\theta - m_a L_c v\dot{\phi}\sin\theta \\ m_a L_c^2 \dot{\phi}^2 \sin\theta\cos\theta + m_a L_c v\dot{\phi}\sin\theta \end{bmatrix}, \tag{40}$$

$$G = \begin{bmatrix} 0 \\ 0 \\ 0 \\ m_a L_c g\cos\theta \end{bmatrix}, \text{ and} \tag{41}$$

$$F = \begin{bmatrix} F_{xrl} + F_{xrr} \\ F_{yrl} + F_{yrr} \\ \frac{1}{2}d(F_{xrl} - F_{yrl}) - b(F_{yrl} + F_{Yrr}) \\ \tau_a \end{bmatrix}. \tag{42}$$

Now, the state variables are defined as $q_1 = (x_e\ y_e\ z_e)^T$, $q_2 = (u\ \dot{\phi}\ \dot{\theta})^T$, and $q = (q_1\ q_2)^T$. Eliminating the tire force terms and rearranging Eqs. (32)–(37), we obtain

$$\dot{q} = \mu + \xi\tau + \delta \tag{43}$$

4. INPUT-OUTPUT LINEARIZATION - THE NONHOLONOMIC MODEL

In this section, we derive the control law for the spatial mobile manipulator based on the model obtained using Eq. (19), the nonholonomic model that neglects tire slip.

We first rewrite Eq. (20) as

$$\ddot{\xi}_u = H + D^{-1}\tau_u \tag{44}$$

where $H = -D^{-1}Q$.

Now, the state variables are defined as

$$\varphi = [\xi_u\ \dot{\xi}_u]. \tag{45}$$

Eqs. (44) and (45) can be used to write

$$\dot{\varphi} = f(\varphi) + g(\varphi)\tau_u. \tag{46}$$

Now we select the output associated with Eq. (46), $y = f(\xi_u)$, as the end-point of the manipulator. Then, differentiating each element of y twice allows terms involving elements of τ_u to appear. Thus, the first and second derivative of the output can be written as

$$\dot{y} = J(\xi_u)\dot{\xi}_u \text{ and} \tag{47}$$

$$\ddot{y} = J(\xi_u)\ddot{\xi}_u + \dot{J}(\xi_u)\dot{\xi}_u. \tag{48}$$

Now, with substitution of Eq. (44), Eq. (48) can be rewritten as

$$\ddot{y} = J(H + D^{-1}\tau_u) + \dot{J}\dot{\xi}_u \tag{49}$$

Then, the input-output description of the system Eq. (46) can be linearized to cancel the nonlinearities in Eq. (49) using the following feedback:

$$\tau_u = F(\varphi) + G(\varphi)u \tag{50}$$

where

$$F(\varphi) = -DJ^{-1}\dot{J}\dot{\xi}_u - DH \text{ and} \tag{51}$$

$$G(\varphi) = -DJ^{-1} \tag{52}$$

Thus, the combined system Eqs. (49)-(52) reduces to

$$\ddot{y} = \gamma \tag{53}$$

The term γ represents a new input to the system which is yet to be chosen. Eq. (53) is known as the double integrator system as it represents n uncoupled double integrators. Control system design of the mobile manipulator is then equivalent to a design problem of decoupled linear subsystems.

5. ROBUST CONTROL – THE DYNAMIC MODEL

For the case of the dynamic model including tire slip, we select the output associated with Eq. (43) as the end point of the mobile manipulator and define the new sets of state variables as $x = (x_1\ x_2)^T$, $x_1 = (x_e\ y_e\ z_e)^T$, and $x_2 = (\dot{x}_e\ \dot{y}_e\ \dot{z}_e)^T$. Then, transformation of the output equation is performed into the global frame. Differentiating the state vector x, we obtain the dynamic equation in the global frame as follows:

$$\dot{x} = \xi(\phi, \theta, x, \delta) + \Phi(\phi, \theta, \delta)\tau + \eta(\phi, \theta, x, \delta) \tag{54}$$

where

$$\Phi(\phi,\theta,\delta) = \begin{bmatrix} 0_{3\times 3} \\ \Gamma(\phi,\theta,\delta) \end{bmatrix} \text{ and} \tag{55}$$

$$\Gamma(\phi,\theta,\delta) = \begin{bmatrix} \cos\phi & -L_a\sin\phi\cos\theta & -L_a\sin\theta\cos\phi \\ \sin\phi & L_a\cos\phi\sin\theta & L_a\sin\phi\sin\phi \\ 0 & 0 & L_a\cos\theta \end{bmatrix} \tag{56}$$

https://doi.org/10.1017/S0263574798000873 Published online by Cambridge University Press

Should the wheel slip be neglected, then the equations of motion can be written as

$$\dot{x}_N = \xi_N(\phi,\theta,x) + \Phi_N(\phi,\theta)\tau. \tag{57}$$

Let us denote the following equations:

$$\Phi(\phi,\theta,\delta) = \Phi_N(\phi,\theta) + \Delta\Phi(\phi,\theta,\delta) \text{ and} \tag{58}$$

$$\xi(\phi,\ \theta,\ x,\ \delta) = \xi_N(\phi,\ \theta,\ x) + \Delta\xi(\phi,\ \theta,\ x,\ \delta) \tag{59}$$

where $\Delta\xi$ and $\Delta\Phi$ are the uncertainty terms. Then, $\Delta\Phi$ can be written as

$$\Delta\Phi(\phi,\ \theta,\ \delta) = \begin{bmatrix} 0_{3\times 3} \\ \Delta\Gamma(\phi,\ \theta,\ \delta) \end{bmatrix}$$

$$= \begin{bmatrix} 0_{3\times 3} \\ \Delta\Gamma_N(\phi,\ \theta) \end{bmatrix} \Delta\Gamma_N^{-1}(\phi,\ \theta)\ \ \Delta\Gamma(\phi,\ \theta,\ \delta)$$

$$= \Phi_N(\phi,\ \theta)\Delta\Gamma_N^{-1}(\phi,\ \theta)\ \ \Delta\Gamma(\phi,\ \theta,\ \delta)$$

$$= \Phi_N(\phi,\ \theta)\tilde{\Phi}(\phi,\ \theta,\ \delta) \tag{60}$$

Similarly, it can be shown that

$$\Delta\xi(\phi,\ \theta,\ x,\ \delta) = \Phi_N(\phi,\ \theta)\ \tilde{\xi}\ (\phi,\ \theta,\ x,\ \delta) \text{ and} \tag{61}$$

$$\Delta\eta(\phi,\ \theta,\ x,\ \delta) = \Phi_N(\phi,\ \theta)\tilde{\eta}(\phi,\ \theta,\ x,\ \delta). \tag{62}$$

Then, ξ, Φ, and η can be rewritten respectively as

$$\xi(\phi,\ \theta,\ x,\ \delta) = \xi_N(\phi,\ \theta,\ x,\ \delta) + \Phi_N(\phi,\ \theta)\tilde{\xi}(\phi,\ \theta,\ x,\ \delta), \tag{63}$$

$$\Phi(\phi,\ \theta,\ \delta) = \Phi_N(\phi,\ \theta) + \Phi_N(\phi,\ \theta)\tilde{\Phi}(\phi,\ \theta,\ \delta), \text{ and} \tag{64}$$

$$\eta(\phi,\ \theta,\ \delta) = \Phi_N(\phi,\ \theta)\tilde{\eta}(\phi,\ \theta,\ \delta). \tag{65}$$

Then, Eq. (54) is rearranged as

$$\dot{x} = \xi_N(\phi,\ \theta,\ x) + \Phi_N(\phi,\ \theta)\tau + \rho(\phi,\ \theta,\ x,\ \delta) \tag{66}$$

where $\rho(\phi,\ \theta,\ x,\ \delta) = \Phi_N(\tilde{\xi}(\phi,\ \theta,\ x,\ \delta) + \tilde{\Phi}(\phi,\ \theta,\ \delta) + \tilde{\eta}(\phi,\ \theta,\ x,\ \delta))$. Note that Eq. (66) is of the form of Eq. (57) with uncertainty from tire slip.

Therefore, the dynamic equations of motion of the mobile manipulator in task space satisfy the matching condition. It is well known that the matching condition is the structural form of a dynamic system to be satisfied for the application of a wide class of robust control algorithms. With this property satisfied, the dynamic model based robust controller is designed based on the variable structure control method. Variable structure control algorithms possess the feature of sliding mode invariance to both system perturbations and external disturbances.[11,12]

Now, the position error and the velocity error are defined as

$$e_p = x_1 - x_1^d \text{ and} \tag{67}$$

$$e_d = x_2 - x_2^d \tag{68}$$

where x_1^d and x_2^d are the desired trajectories. Then, the tracking error dynamics can be described as follows:

$$\dot{e} = Ae + B\{\chi + \eta - \dot{x}_2^d\} \tag{69}$$

where

$$e = (e_p\ e_d)^T \tag{70}$$

The principle of the variable structure control method is to design a control law to make the system reach the following manifold:

$$S(e) = C_e = [C_p\ C_d] = \begin{bmatrix} e_p \\ e_d \end{bmatrix} \tag{71}$$

Once the system reaches the switching manifold, it will remain on it, which is said to be in the sliding mode. If C_d is nonsingular, we have

$$\dot{e}_p + C_d^{-1}C_p e_p = 0 \tag{72}$$

One of the conditions that ensures that the switching manifold is reached can be described as

$$S^T\dot{S} < 0. \tag{73}$$

Variable structure control usually takes the following form:

$$\chi = \chi_e + \Delta\chi \tag{74}$$

where χ_e is the equivalent sliding mode input, and $\Delta\chi$ is the additional term to satisfy the reaching conditions.

Now, the matrix C in the switching manifold is set to be

$$C = [C_p\ C_d] = [\Lambda\ I] \tag{75}$$

where $\Lambda = \text{diag}[\lambda_1\ \lambda_2]$, $(\lambda_1,\ \lambda_2 > 0)$. Then, the sliding mode for the system can be written as

$$\dot{e}_p = -\Lambda e_p \tag{76}$$

which shows the exponential convergence of the tracking error. Now, we need to determine the control law for the dynamic system to guarantee the reaching condition. Taking the time derivative in the reaching condition along the trajectory of the system, we obtain

$$S^T\dot{S} = S^T(CSe + \chi + \rho). \tag{71}$$

The control design to follow is based on the premise that it may be possible to estimate the norm bounds on its effect on the tracking performance of the system. The control law χ is then designed to guarantee stability of Eq. (69). The norm bound of the uncertainty term ρ is obtained as

$$\| \rho \| = \| \Phi_N(\tilde{\xi} + \tilde{\Phi} + \tilde{\eta}) \| \le \bar{\rho}. \tag{78}$$

Then, it is not difficult to determine χ which satisfies the reaching condition as follows:

$$\chi = -\Lambda e_d - \Delta\chi \tag{79}$$

where

$$\Delta\chi = \begin{cases} \dfrac{S}{\| S \|}\bar{\rho}, & \text{for } \| S \| \neq 0 \\ 0, & \text{for } \| S \| = 0 \end{cases}. \tag{80}$$

Substituting Eqs. (79) and (80) into Eq. (77), it is seen that when $\| S \| \neq 0$,

$$\begin{aligned} S^T\dot{S} &= -\| S \|\bar{\rho} + S^T\rho \\ &\le -\| S \|\bar{\rho} + \| S \|\ \| \rho \| \\ &= -\| S \|(\bar{\rho} + \| \rho \|) \\ &< 0. \end{aligned} \tag{81}$$

https://doi.org/10.1017/S0263574798000873 Published online by Cambridge University Press

Because the tracking error is governed by Eq. (69) on the switching surface, the tracking error converges exponentially to zero when the sliding mode is reached. Therefore, the above control law is the variable structure control of the mobile manipulator. Now, selecting $C_p = I$ and $C_d = \Lambda$, the error dynamics are written as

$$\begin{bmatrix} \dot{e}_p \\ \dot{e}_d \end{bmatrix} = \begin{bmatrix} -\Lambda & 0 \\ 0 & -\Lambda \end{bmatrix} \begin{bmatrix} e_p \\ e_d \end{bmatrix}. \tag{82}$$

In practice, variable structure controllers result in input chattering because high frequency switching action is required in generating the control input. One common method to overcome the chattering is to modify Eq. (80) as follows:

$$\Delta\chi = \begin{cases} \dfrac{S}{\|S\|}\bar{\rho}, \text{ for } \|S\| > \epsilon \\ \dfrac{S}{\rho}\bar{\rho}, \text{ for } \|S\| \le 0 \end{cases}. \tag{83}$$

where $0 < \epsilon \le 1$.

6. SIMULATIONS

In this section, computer simulation is conducted to examine the performance of the tracking controller designed for each model of the mobile manipulator developed throughout this paper. The parameters used in the simulations are $m_p = 300$ kg, $m_a = 50$ kg, $I_p = 30$ kg·m^2, and $I_a = 10$ kg·m^2 where m_p is the mass of the platform, m_a is the mass of the arm, I_p is the moment of inertia of the platform, and I_a is the moment of the inertia of the manipulator. The longitudinal and lateral tire coefficients, C_x and C_y, are both set to 40034 N/rad.

The following desired trajectory is used in the simulation:

$$x_d(t) = 3 + \sin t$$
$$y_d(t) = 3 + \cos t$$
$$z_d(t) = 0.6854 + 0.1 \sin t$$

In this simulation, the mobile manipulator is initially at rest and the initial position of the end-effector is set to (3.3, 4.3, 0.7854) which is not on the desired trajectory. In simulation, the end-point of the mobile manipulator is commanded to follow the desired trajectory and the platform is responsible for positioning the manipulator at a specified point in the workspace to avoid singular configurations of the system. The desired trajectory follows a circle in the *xy* plane with a sinusoidal variation in the z direction. The mobile platform is ordered to adjust its heading in a sinusoidal manner to accommodate for the effects of the manipulator motion in the *xy* plane due to the combination of the manipulator's vertical movements and the platform's yaw. Figure 4 shows the desired trajectory of the end-point of the manipulator in task space. Figure 5 shows the tracking errors of the nonholonomic model based controller in task space and demonstrates the excellent tracking performance as expected.

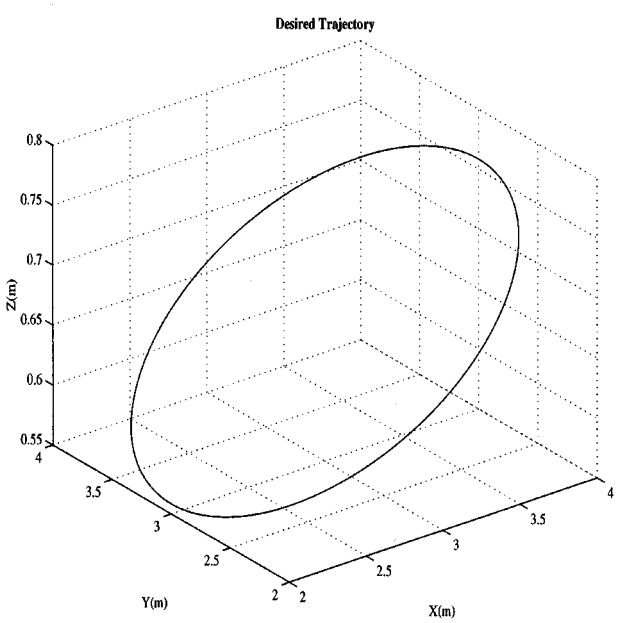


Fig. 4. The desired trajectory.

Many conditions exists for which the nonholonomic model is insufficient. That is, inertial and/or external loads can only be overcome with appreciable wheel slip. Figure 6 depicts the best tuned tracking performance of the input-output linearizing controller for the mobile manipulator subject to wheel slip. It is obvious that the tracking performance of this controller, which was designed based on the wheel rolling condition, degrades significantly in the presence of wheel slip. Figure 7 shows the tracking performance of the variable structure controller designed for the realistic model of the mobile manipulator. Λ is set to diag(0.5 0.5 0.5). It is observed that the tracking errors quickly converge to very small values compared to the non-robust control design.

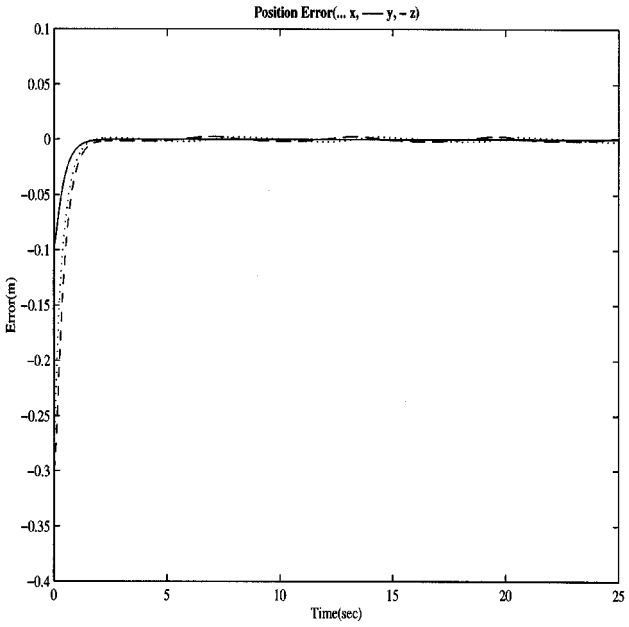


Fig. 5. Position error - the nonholonomic model.

https://doi.org/10.1017/S0263574798000873 Published online by Cambridge University Press

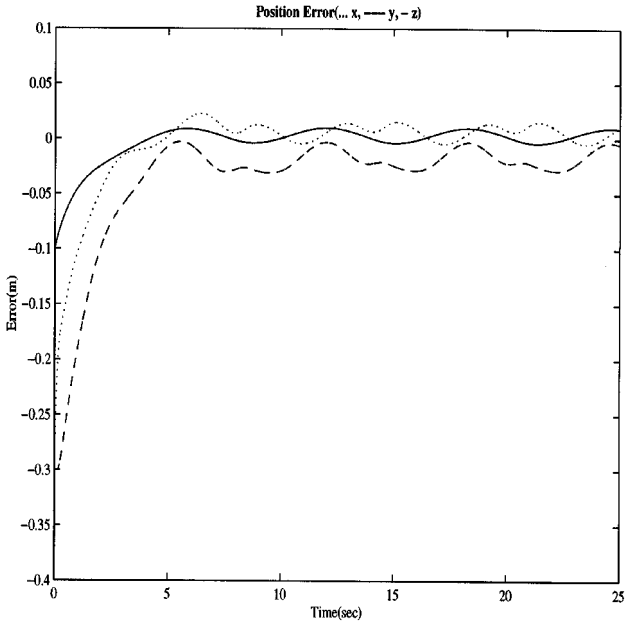


Fig. 6. Position error without robust control - the dynamic model.

7. CONCLUSION

In this paper, we have developed the nonholonomic equations of motion of a mobile manipulator using a Lagrange-d'Alembert formulation. In this formulation, the equations of motion are projected onto the subspace of allowable motions. Then, the dynamic model of the mobile manipulator was developed for high load and high speed applications, in which Dugoff's tire friction model was incorporated. For the nonholonomic model, the input-output linearization method was utilized to solve the tracking problem. This control approach provided excellent tracking control for a system for which the wheel rolling condition is valid. However, for highly loaded systems, wheel slip is necessary, and the effect of wheel slip on the position tracking was identified in the simulation. Based on the degraded performance of the input-output linearization approach, a robust controller was designed to eliminate the harmful effects of the wheel slip which was shown to act as a disturbance to the system. The effectiveness of the realistic model based robust controller was then demonstrated through computer simulation.

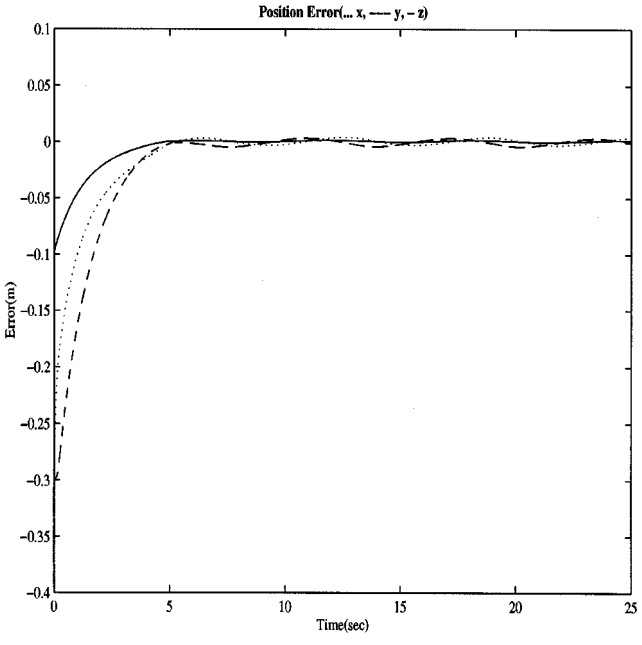


Fig. 7. Position error with robust control - the dynamic model.

References

1. F.D. Boyden and S.A. Velinsky, "Dynamic modeling of wheeled mobile robots for high load applications" *Proceedings of IEEE International Conference on Robotics and Automation* (1994) pp. 3071–3078.
2. N.A.M. Hootsmanns and S. Dubowsky, "The motion control of manipulators on mobile vehicles" *Proceedings of IEEE International Conference on Robotics and Automation* (1991) pp. 2336–2341.
3. K. Liu and F.L. Lewis, "Decentralized continuous robust controller for mobile robots" *Proceedings of IEEE International Conference on Robotics and Automation* (1990) pp. 1822–1827.
4. W.M. Jang and G.J. Wiens, "Passive joint control of dynamic coupling in mobile robots" *Int. J. Robotics Research* **3**, 209–220 (1994).
5. Y. Yamamoto and X. Yun, "Modeling and compensation of the dynamic interaction of a mobile manipulator" *Proceedings of IEEE International Conference on Robotics and Automation* (1994) pp. 2184–2192.
6. J.H. Chung, S.A. Velinsky and R.A. Hess, "Interaction control of a redundant mobile manipulator" *Int. J. Robotics Research* (to appear).
7. G.J. Weins, "Effect of dynamic coupling in mobile robotic systems" *Proceedings of SME Robotic Research World Conference* (1989) pp. 43–57.
8. A. Ghamsepoor and N. Sepehri, "A measure of machine stability for moving base manipulators" *Proceedings of IEEE International Conference on Robotics and Automation* (1995) pp. 2249–2254.
9. F.G. Pin, J.C. Culioli and D.B. Reister, "Using minimax approaches to plan optimal task commutation configurations for combined mobile platform-manipulator systems" *IEEE Transactions on Robotics and Automation* **10**(1), 44–54 (1994).
10. H. Dugoff, P. Fancher and L. Segal, "An analysis of tire traction properties and their influence on vehicle dynamic performance" *SAE Transaction* 1219–1243 (1970).
11. V.I. Utkin, *Sliding Modes in Control Optimization* (Springer-Verlag, Berlin, 1992).
12. K.D. Young, *Variable Structure Control for Robotics and Aerospace Applications* (Elsevier, Amsterdam, 1993).

https://doi.org/10.1017/S0263574798000873 Published online by Cambridge University Press